Available online at www.sciencedirect.com
ScienceDirect
Phytochemistry 69 (2008) 1653–1660
PHYTOCHEMISTRY
www.elsevier.com/locate/phytochem

Pokeweed antiviral protein region Gly209–Lys225 is critical for RNA *N*-glycosidase activity of the prokaryotic ribosome

Yoshimi Nagasawa, Kazuyuki Fujii, Takafumi Yoshikawa, Yoshinori Kobayashi, Toshiya Kondo *

School of Pharmaceutical Sciences, Kitasato University, 5-9-1 Shirokane, Minato-ku, Tokyo 108-8641, Japan

Received 4 December 2007; received in revised form 12 February 2008
Available online 2 April 2008

Abstract

Pokeweed antiviral protein (PAP) isolated from *Phytolacca americana* is a ribosome-inactivating protein (RIP) that has RNA *N*-glycosidase (RNG) activity towards both eukaryotic and prokaryotic ribosomes. In contrast, karasurin-A (KRN), a RIP from *Trichosanthes kirilowii* var. *japonica*, is active only on eukaryotic ribosomes. Stepwise selection of chimera proteins between PAP and KRN indicated that the C-terminal region of PAP (residues 209–225) was critical for RNG activity toward prokaryotic ribosomes. When the region of PAP (residues 209–225) was replaced with the corresponding region of KRN the PAP chimera protein, like KRN, was active only on eukaryotic ribosomes. Furthermore, insertion of the region of PAP (residues 209–225) into the KRN chimera protein resulted not only in the detectable RNG activity toward prokaryotic ribosome, but also activity toward the eukaryotic ribosomes as well that was seven-fold higher than for the original KRN. In this study, the possibility of genetic manipulation of the activity and substrate specificity of RIPs is demonstrated.

Keywords: Pokeweed; *Phytolacca americana*; *Phytolaccaceae*; Ribosome-inactivating protein; RNA *N*-glycosidase; Substrate specificity; Chimera protein; Prokaryotic ribosome; Pokeweed antiviral protein; Karasurin-A

1. Introduction

Ribosome-inactivating proteins (RIPs) are widely distributed in higher plants and belong to a group of RNA *N*-glycosidases (RNG, EC 3.2.2.22), which remove a specific adenine residue from a highly conserved α-sarcin/ricin loop of the large rRNA (Endo et al., 1987; Endo and Tsurugi, 1987; Girbés et al., 2004). Removal of the adenine residue induces a conformational change that prevents binding of elongation factor 2 to the ribosome; this interrupts translation and results in cell death due to protein synthesis arrest (Moazed et al., 1988).

Based on the structural properties and their corresponding genes, RIPs are currently divided into three groups (Peumans et al., 2001). Type I RIPs, such as pokeweed antiviral protein (PAP) isolated from leaves of *Phytolacca americana* (Irvin, 1975) and karasurin-A (KRN) isolated from root tubers of *Trichosanthes kirilowii* var. *japonica* (Toyokawa et al., 1991), are basic proteins of approximately 30 kDa consisting of a single polypeptide chain. To date, most RIPs have been classified as type I RIPs (Barbieri et al., 1993). Type II RIPs, such as ricin from castor bean seeds, consist of a single polypeptide chain (A-chain) and a galactose-binding B-chain linked by a disulfide linkage (Olsnes, 2004). The A-chain is equivalent to a type I RIP. Type III RIPs are a single chain containing an extended carboxyl-terminal domain of an unknown function (Reinbothe et al., 1994).

RIPs have attracted the interest of researchers due to their possible use anti-cancer drugs, anti-HIV drugs and agrichemicals because of their cytocidal properties and broad-spectrum antiviral activities (Parikh and Tumer, 2004). For therapy of cancer and AIDS, PAP has been

* Corresponding author. Tel.: +81 3 5791 6239; fax: +81 3 3444 6192.
E-mail address: kondout@pharm.kitasato-u.ac.jp (T. Kondo).

0031-9422/$ - see front matter © 2008 Elsevier Ltd. All rights reserved.
doi:10.1016/j.phytochem.2008.02.012

used as an immunotoxin conjugated to a variety of monoclonal antibodies (Zarling et al., 1990; Ek et al., 1998; Uckun et al., 1999; Qi et al., 2004), although the molecular mechanism of the action is still unclear.

Comparison of amino acid sequences among RIPs has revealed a number of highly conserved residues, such as Tyr^{80}, Tyr^{123}, Glu^{177} and Arg^{180} in ricin (Ready et al., 1988). The functional role of these amino acid residues in the RNG activity has been elucidated using both X-ray crystallographic structural analyses and site-directed mutagenetic studies. The X-ray crystallographic structure of ricin was the first RIP to be determined (Montfort et al., 1987); since then the structures of other RIPs have been found to be similar to that of ricin. Crystallographic analysis of ricin complexes with various ligands has resulted in the proposal that Tyr^{80} and Tyr^{123} sandwich the target adenine ring, with the side chain of Arg^{180} protonating the N-3 atom of the adenine ring, whilst the negative charge of Glu^{177} stabilizes the positive oxocarbonium transition state (Monzingo and Robertus, 1992). Mutational analysis of these amino acid residues has confirmed their importance in RNG activity (Frankel et al., 1990; Ready et al., 1991).

Among the different biological species, the adenine targeted by RIPs universally conserves in an α-sarcin/ricin loop of the largest RNA (Endo and Tsurugi, 1988). RIPs remove the A4324 in the eukaryotic 28S rRNA of rat liver ribosomes, equivalent to the A2660 in the prokaryotic 23S rRNA of *Escherichia coli* ribosomes. In general, while RIPs exhibit RNG activity toward eukaryotic ribosomes, only a few RIPs are active on prokaryotic ribosomes. PAP is active on eukaryotic as well as on prokaryotic ribosomes (Hartley et al., 1991). This is in marked contrast with KRN, which exhibits activity only toward eukaryotic ribosomes. However, there are only a few studies on substrate specificity reported to date (Chaddock et al., 1996). The factors determining such specificity of RIPs thus remain to be elucidated.

In order to identify the amino acid residues or the region that contributes to the selective RNG activity toward prokaryotic ribosomes, we constructed a series of PAP and KRN chimera proteins substituting corresponding regions of the respective proteins, and examined changes in selectivity of RNG activities toward eukaryotic and prokaryotic ribosomes. The results are discussed below.

2. Results

2.1. The RNG activities of PAP and KRN chimera proteins

We prepared chimera proteins of two ribosome-inactivating proteins (RIPs), pokeweed antiviral protein (PAP), active on both eukaryotic and prokaryotic ribosomes, and karasurin-A (KRN), active on eukaryotic ribosomes only. In general, RIPs from different genera and families show relatively low levels of sequence identity (Robertus, 1991; Barbieri et al., 1993), but two consecutively matched regions, the active site and RNA binding domain, are highly conserved among the RIPs (Hudak et al., 2004; Baykal and Tumer, 2007). Although PAP and KRN share only 28% sequence identity, the active site and RNA binding domain were well conserved in the sequences (Fig. 1). Therefore, these two regions were used as an overlap for the chimera proteins, which consequently divided into three domains, the N-terminal domain (PAP residues 1–74), the central domain (PAP residues 75–177) and the C-terminal domain (PAP residues 178–262). The chimera proteins, P1, P2, P3, K1, K2 and K3, were constructed by exchanging one of the domains of PAP and KRN with the other (Fig. 2). The RNA *N*-glycosidase (RNG) activities of chimera proteins toward eukaryotic and prokaryotic ribosomes were estimated using the half maximal effective concentration (EC_{50}) for the cleavage of ribosomes. The EC_{50} values are shown in Table 1. Although the RNG

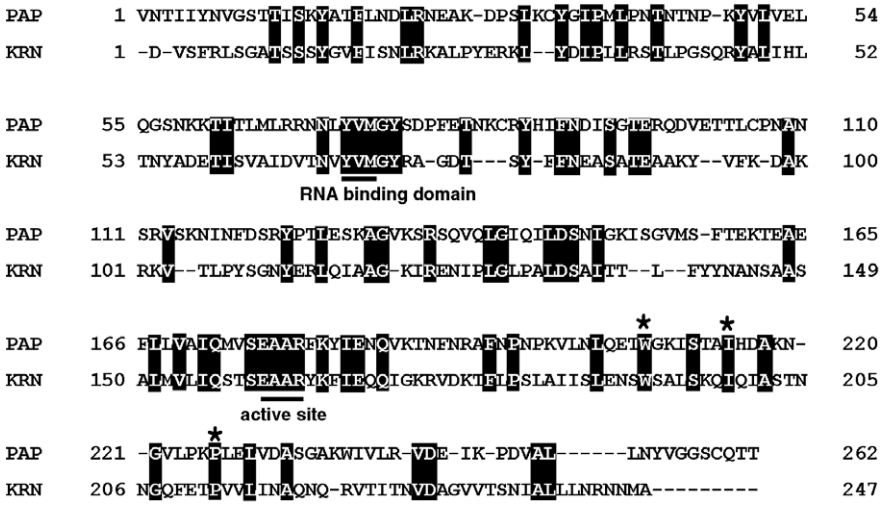

Fig. 1. Alignment of amino acid sequences of PAP and KRN. The identical amino acid residues between PAP and KRN are shaded in black. The active site and RNA binding domain are underlined. Asterisks indicate the amino acids at the junction to construct chimera proteins.

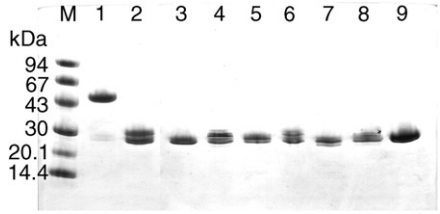

Fig. 2. SDS-PAGE of recombinant proteins. The proteins were separated on 8–25% SDS-polyacrylamide gradient gel, and the gel was stained with Coomassie Blue. Lane M contains molecular weight markers (molecular weights in kDa given at the left). Lane 1 shows purified recombinant PAP (rPAP)–glutathione *S*-transferase (GST) fusion protein on GSTrap FF column. Lanes 2–9 indicate recombinant proteins after PreScission protease cleavage of rPAP, recombinant KRN (rKRN), P1, P2, P3, K1, K2 and K3, respectively. GST, rPAP, rKRN and chimera proteins (P1–3 and K1–3) had the molecular weight of 27, 29, 27 and 27–29 kDa, respectively. The bands of rKRN, P2, K1 and K3 were overlapped with that of GST.

activity of recombinant KRN (rKRN) toward eukaryotic ribosomes was higher than that of recombinant PAP (rPAP), rKRN showed no cleavage to prokaryotic ribosome even at the highest concentration tested, i.e. 12,000 nM. Chimera protein P3, with the C-terminal region of KRN, lost its RNG activity toward prokaryotic ribosomes, although the activity toward eukaryotic ribosomes was higher than P1 and P2. Correspondingly, chimera proteins K3, with the C-terminal region of PAP, acquired RNG activity toward prokaryotic ribosomes, although the RNG activity toward eukaryotic ribosomes of K3 was 75-fold or 4800-fold weaker than K1 or rKRN, respectively. These results suggested that the C-terminal region of PAP is essential for activity toward prokaryotic ribosomes.

2.2. The RNG activity of PAP chimera proteins P4–9 partially exchanged at the C-terminal domain

As shown in Table 1B, PAP chimera proteins were constructed by partially swapping the C-terminal domain and examining their RNG activities. The C-terminal domain of PAP was divided into three sections at conserved amino acids Trp^{208} and Pro^{226}, and these sections of PAP were replaced with the corresponding regions of KRN to obtain chimera proteins from P4 to P7. With respect to eukaryotic ribosomes, no notable differences in the EC_{50} values for P4 and P5 were observed. The RNG activity of P5 toward eukaryotic ribosomes was about half that of rPAP, whereas the RNG activity of P5 toward prokaryotic ribosomes was stronger than rPAP. On the other hand, P4 showed no cleavage of prokaryotic ribosomes even at 12000 nM. P6 and P7 exhibited RNG activity toward eukaryotic ribosomes, but their activity was 51- and 210-fold weaker than rPAP, respectively. With respect to prokaryotic ribosomes, the RNG activity of P6 was 99-fold weaker than that of rPAP, whilst P7 showed no activity. Taken together, these results demonstrated that the region of PAP from residues 209 to 225 is required for RNG activity toward prokaryotic ribosomes.

The determined region was divided at amino acid Ile^{215} common to PAP and KRN. Each section was replaced in turn with the corresponding region of KRN, and chimera proteins P8 and P9 were constructed. Neither P8 nor P9 lost RNG activity toward prokaryotic ribosomes by replacing either region of PAP (residues 216–225) or (residues 209–214) with the corresponding regions of KRN.

2.3. The RNG activity of KRN chimera proteins K4–7 partially exchanged at the C-terminal domain

In order to confirm the role of the region of PAP (residues 209–225), two types of KRN chimera proteins were constructed. K4 and K7 contained the region of PAP (residues 209–225) in place of KRN (residues 193–211), whereas K5 and K6 did not. All four chimera proteins exhibited RNG activity toward eukaryotic ribosomes, and interestingly, the RNG activity of K7 was seven-fold higher than rKRN (Table 1C). As for the RNG activities toward prokaryotic ribosomes, K4 and K7 acquired obvious cleavage activities, whereas K5 and K6 showed no cleavage activity at the same concentration, i.e. 12,000 nM. The relative RNG activities toward prokaryotic ribosomes of K4 and K7 were 26% and 44% in comparison with rPAP, respectively. Thus, RNG activity toward prokaryotic ribosomes can be produced in KRN by the introduction of the region of PAP (residues 209–225).

3. Discussion

PAP chimera protein P7, in which the region of PAP (residues 209–225) was replaced with the corresponding region KRN, was not active on prokaryotic ribosomes. But P8 and P9, in which the portion of PAP (residues 209–226) was replaced with the corresponding region of KRN, retained RNG activity toward prokaryotic ribosomes. Furthermore, single amino acid substitution mutants of Gly^{209}, Lys^{210}, Ile^{211}, Thr^{213}, Ala^{214}, His^{216}, Asp^{217}, Lys^{219}, Asn^{220} and Lys^{225} in the region of PAP (residues 209–225) to alanine or the corresponding residue of KRN did not alter selectivity toward prokaryotic ribosomes of rPAP (data not shown). These results suggest that the region of PAP (residues 209–225) is critical for RNG activity toward prokaryotic ribosomes and two or more discontinuous amino acid residues in this region participate in the substrate specificity.

The X-ray crystallographic structure of PAP was elucidated (Monzingo et al., 1993), and indicated that the region of PAP (residues 209–225) is located at the surface of the protein and contains an α helix (Fig. 3). Structural and mutagenetic studies of PAP suggest that the active site residues, Tyr^{72}, Tyr^{123}, Glu^{176} and Arg^{179}, directly participate in RNG activity and that the active center cleft residues, Asn^{69}, Phe^{90}, $Asn^{91}$and Asp^{92} are important in binding to ribosomes via the ribosomal protein L3 (Rajamohan et al., 2001). Since the region of PAP (residues 209–225)

Table 1
Schematic structures and the RNA *N*-glycosidase activities of recombinant proteins

Recombinant proteins	EC_{50}[a] value (nM)	
	Eukaryotic ribosomes	Prokaryotic ribosomes
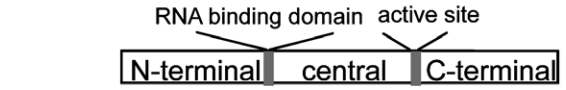		
	0.87 0.014	8.6 NA[b]
(A)		
P1	240	2500
P2	68	140
P3	50	NA
K1	0.89	NA
K2	97	NA
K3	67	280
(B)		
P4	1.5	NA
P5	1.6	5.4
P6	44	850
P7	180	NA
P8	57	180
P9	160	1000
(C)		
K4	0.14	>12000
K5	21	NA
K6	2.7	NA
K7	0.0021	>12000

Sequences from PAP are shown in black bars and from KRN in white bars. Number of residues at the junction of PAP and KRN are indicated. (A) Structures of the chimera proteins in which the N-terminal domain, the central domain and the C-terminal domain of PAP or KRN replace the corresponding domain of each protein. (B) Structures of the chimera proteins substituted a partial region of the C-terminal domain of PAP by those of KRN. (C) Structures of the chimera proteins substituted a partial region of the C-terminal domain of KRN by those of PAP.

[a] EC_{50}, effective concentrations which cause 50% cleavage of eukaryotic and prokaryotic ribosomes.

[b] NA, no activity even up to 12,000 nM.

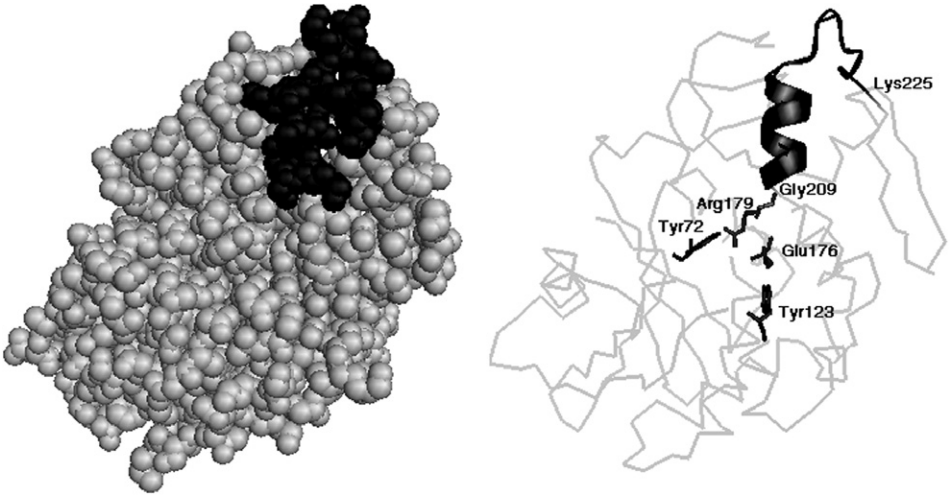

Fig. 3. The X-ray crystallographic structure of PAP (PDB 1PAF). Left: PAP are displayed as spheres, and the region of PAP (residues 209–225) are in black. Right: The region of PAP (residues 209–225) is shown as black cartoon model. The active site residues of PAP including Tyr^{72}, Tyr^{123}, Glu^{176} and Arg^{179}, which are shown as black stick model, are critical in catalysis.

do not contain these residues, we anticipate that substrate specificity may be controlled by a different mechanism to RNG activity.

There is a clear difference in the number of charged residues between the region of PAP (residues 209–225) and the corresponding region of KRN. The active region of PAP has five charged amino acids, Lys^{210}, His^{215}, Asp^{216}, Lys^{219} and Lys^{225}, whereas the corresponding region of KRN has only two charged amino acids, i.e. Lys^{197} and Glu^{210}. Thus, charge density may affect the selectively of RNG activity toward the prokaryotic ribosomes.

To determine the region contributing to selective RNG activity toward prokaryotic ribosomes, a series of PAP and KRN chimera proteins were constructed and their RNG activities examined toward eukaryotic and prokaryotic ribosomes. KRN chimera proteins were found to show stronger activity compared to the correlative PAP chimera proteins with the exception of P5 and K5, in which the region of PAP (178–207) and the corresponding region of KRN were exchanged. This implies that amino acids within either this region of PAP (residues 178–207) or the corresponding region of KRN may participate in RNG activity. Furthermore, K7 in which the PAP region (residues 209–225) was introduced exhibited a seven-fold higher activity toward eukaryotic ribosomes than rKRN. To date, there are few reports of mutant proteins with enhanced RNG activity. These results were not obtained using single amino acid substitutions but rather from using chimera proteins where particular domains were exchanged. This strategy could thus be useful for creating mutant proteins with enhanced RNG activity as well as for analyzing substrate specificity.

4. Conclusions

In this study, we have determined a region of PAP which plays a crucial role in substrate specificity. In addition, we have succeeded in intensifying RNG activity toward eukaryotic ribosome in chimera protein K7 by introducing the region of PAP (residues 209–225). It is hoped that this approach to RIPs will lead to novel applications, giving higher substrate specificity and a lesser toxic side effects.

5. Experimental

5.1. Construction of expression plasmids

Genomic DNA prepared from spring leaves of *P. americana* and plasmid pMAL-c2 containing the coding region of KRN (Mizukami et al., 2001) were used as templates to amplify the fragments encoding PAP and KRN by PCR. PCR primers were designed based on the nucleotide sequences of *PAP* (Accession no. AY572976) and *KRN* (Accession no. AB000666), as shown in Table 2. The sense primers included a restriction site for *Bam*HI at the 5′-end, and the antisense primers included a stop codon and restriction site for *Sma*I at the 3′-end. For construction of chimera proteins, two rounds of PCR were carried out. The PCR fragments of *PAP* and *KRN* were used for the first PCR template. In the first step, two PCR fragments, F1 and F2, were amplified with the templates and primer pairs listed in Table 2. The second step PCR was templated using the first step PCR fragments F1 and F2 with the sense primer of F1 and antisense primer of F2. The PCR fragment and the pGEX-6P-1 vector were digested with *Bam*HI and *Sma*I, and ligated to produce the cDNA clone of the chimera protein genome. The DNA sequence of the final construct was verified using sequencing analysis with the BigDye Terminator v.3.0 Cycle Sequencing Kit and ABI PRISM 3100 Genetic Analyzer (Applied Biosystems, Foster City, CA).

Table 2
Primers and templates used for the construction of PAP and KRN chimera proteins

PAP	Sense	5′-ACTGGATCCGTGAATACAATCATCTACAAT-3′	
	Antisense	5′-ATTTCCCGGGTCAAGTTGTCTGACAGCTCCC-3′	
	Template	Genomic DNA from spring leaves of *Phytolacca americana*	
KRN	Sense	5′-ACTGGATCCGATGTTAGCTTCCGTTTATCAGGT-3′	
	Antisense	5′-ATTTCCCGGGTCATGCCATATTGTTTCTATT-3′	
	Template	Plasmid pMAL-c2 containing the coding region of KRN	
		F1	F2
P1	Sense	5′-ACTGGATCCGATGTTAGCTTCCGTTTATCAGGT-3′	5′-GACGTAACGAACGTCTATGTGATGGGTTAT-3′
	Antisense	5′-ATAACCCATCACATAGACGTTCGTTACGTC-3′	5′-ATTTCCCGGGTCAAGTTGTCTGACAGCTCCC-3′
	Template	The PCR fragment of KRN	The PCR fragment of PAP
P2	Sense	5′-ACTGGATCCGTGAATACAATCATCTACAAT-3′	5′-CTCATTCAGTCGACGTCAGAGGCAGCAAGA-3′
	Antisense	5′-TCTTGCTGCCTCTGACGTCGACTGAATGAG-3′	5′-ATTTCCCGGGTCAAGTTGTCTGACAGCTCCC-3′
	Template	The PCR fragment of K1	The PCR fragment of PAP
P3	Sense	5′-ACTGGATCCGTGAATACAATCATCTACAAT-3′	5′-GCCATACAAATGGTATCTGAGGCTGCGAGG-3′
	Antisense	5′-CCTCGCAGCCTCAGATACCATTTGTATGGC-3′	5′-ATTTCCCGGGTCATGCCATATTGTTTCTATT-3′
	Template	The PCR fragment of PAP	The PCR fragment of KRN
K1	Sense	5′-ACTGGATCCGTGAATACAATCATCTACAAT-3′	5′-AGACGAAACAATTTGTATGTTATGGGATAT-3′
	Antisense	5′-ATATCCCATAACATACAAATTGTTTCGTCT-3′	5′-ATTTCCCGGGTCATGCCATATTGTTTCTATT-3′
	Template	The PCR fragment of PAP	The PCR fragment of KRN
K2	Sense	5′-ACTGGATCCGATGTTAGCTTCCGTTTATCAGGT-3′	5′-GCCATACAAATGGTATCTGAGGCTGCGAGG-3′
	Antisense	5′-CCTCGCAGCCTCAGATACCATTTGTATGGC-3′	5′-ATTTCCCGGGTCATGCCATATTGTTTCTATT-3′
	Template	The PCR fragment of P1	The PCR fragment of KRN
K3	Sense	5′-ACTGGATCCGATGTTAGCTTCCGTTTATCAGGT-3′	5′-CTCATTCAGTCGACGTCAGAGGCAGCAAGA-3′
	Antisense	5′-TCTTGCTGCCTCTGACGTCGACTGAATGAG-3′	5′-ATTTCCCGGGTCAAGTTGTCTGACAGCTCCC-3′
	Template	The PCR fragment of KRN	The PCR fragment of PAP
P4	Sense	5′-ACTGGATCCGTGAATACAATCATCTACAAT-3′	5′-AGTTTGGAAAATAGTTGGGGTAAGATTTCA-3′
	Antisense	5′-GGAGAGAGCAGACCATGTCTCTTGCAAATT-3′	5′-ATTTCCCGGGTCATGCCATATTGTTTCTATT-3′
	Template	The PCR fragment of PAP	The PCR fragment of KRN
P5	Sense	5′-ACTGGATCCGTGAATACAATCATCTACAAT-3′	5′-AATTTGCAAGAGACATGGTCTGCTCTCTCC-3′
	Antisense	5′-TGAAATCTTACCCCAACTATTTTCCAAACT-3′	5′- ATTTCCCGGGTCAAGTTGTCTGACAGCTCCC-3′
	Template	The PCR fragment of P3	The PCR fragment of PAP
P6	Sense	5′-ACTGGATCCGTGAATACAATCATCTACAAT-3′	5′-GGAGTTTTACCCAAACCTGTTGTGCTTATA-3′
	Antisense	5′-TATAAGCACAACAGGTTTGGGTAAAACTCC-3′	5′-ATTTCCCGGGTCATGCCATATTGTTTCTATT-3′
	Template	The PCR fragment of PAP	The PCR fragment of KRN
P7	Sense	5′-ACTGGATCCGTGAATACAATCATCTACAAT-3′	5′-GGACAGTTTGAAACTCCTCTCGAGCTAGTG-3′
	Antisense	5′-CACTAGCTCGAGAGGAGTTTCAAACTGTCC-3′	5′- ATTTCCCGGGTCAAGTTGTCTGACAGCTCCC-3′
	Template	The PCR fragment of P4	The PCR fragment of PAP
P8	Sense	5′-ACTGGATCCGTGAATACAATCATCTACAAT-3′	5′- AAGATTTCAACAGCAATTCAGATAGCGAGT-3′
	Antisense	5′-ACTCGCTATCTGAATTGCTGTTGAAATCTT-3′	5′-ATTTCCCGGGTCAAGTTGTCTGACAGCTCCC-3′
	Template	The PCR fragment of PAP	The PCR fragment of P7
P9	Sense	5′-ACTGGATCCGTGAATACAATCATCTACAAT-3′	5′-GCTCTCTCCAAGCAAATTCATGATGCCAAG-3′
	Antisense	5′-CTTGGCATCATGAATTTGCTTGGAGAGAGC-3′	5′- ATTTCCCGGGTCAAGTTGTCTGACAGCTCCC-3′
	Template	The PCR fragment of P7	The PCR fragment of PAP
K4	Sense	5′- ACTGGATCCGATGTTAGCTTCCGTTTATCAGGT-3′	5′- AGTTTGGAAAATAGTTGGGGTAAGATTTCA-3′
	Antisense	5′-TGAAATCTTACCCCAACTATTTTCCAAACT-3′	5′-ATTTCCCGGGTCAAGTTGTCTGACAGCTCCC-3′
	Template	The PCR fragment of KRN	The PCR fragment of PAP
K5	Sense	5′-ACTGGATCCGATGTTAGCTTCCGTTTATCAGGT-3′	5′-AATTTGCAAGAGACATGGTCTGCTCTCTCC-3′
	Antisense	5′-GGAGAGAGCAGACCATGTCTCTTGCAAATT-3′	5′-ATTTCCCGGGTCATGCCATATTGTTTCTATT-3′
	Template	The PCR fragment of K3	The PCR fragment of KRN
K6	Sense	5′-ACTGGATCCGATGTTAGCTTCCGTTTATCAGGT-3′	5′-GGACAGTTTGAAACTCCTCTCGAGCTAGTG-3′
	Antisense	5′-CACTAGCTCGAGAGGAGTTTCAAACTGTCC-3′	5′-ATTTCCCGGGTCAAGTTGTCTGACAGCTCCC-3′
	Template	The PCR fragment of KRN	The PCR fragment of PAP
K7	Sense	5′-ACTGGATCCGATGTTAGCTTCCGTTTATCAGGT-3′	5′-GGAGTTTTACCCAAACCTGTTGTGCTTATA-3′
	Antisense	5′-TATAAGCACAACAGGTTTGGGTAAAACTCC-3′	5′-ATTTCCCGGGTCATGCCATATTGTTTCTATT-3′
	Template	The PCR fragment of K4	The PCR fragment of KRN

F1 and F2 are the first step PCR fragments amplified by the primers and template listed below. Underlines indicate the restriction sites for *Bam*HI and *Sma*I.

5.2. Expression and purification of recombinant proteins

E. coli XL1-Blue cells transformed with the expression plasmid were grown at 37 °C for 16 h in 10 ml LB medium supplemented with 50 mg/ml carbenicillin (LB/Cb). The culture were transferred to fresh 250 mL LB/Cb and then incubated at 37 °C until the OD_{600} reached 0.5–0.7. Once this density was reached, protein expression was induced with 1 mM isopropyl-1-thio-β-D-galactopyranoside and carried out for an additional 45 h at 12 °C. Cells were collected using centrifugation at 10,000*g* for 5 min, washed once with TE buffer, and resuspended in 20 ml sonication buffer (50 mM Tris–HCl, 50 mM NaCl, 1 mM EDTA, 1 mM DTT, pH 8.0) containing 10 μg/ml lysozyme. After incubation at 30 °C for 15 min, cells were sonicated three times for 30 s with 2 s intervals at 70% power (Astrason Sonicator XL2020, Misonix Inc.) on ice. The cell lysates were centrifuged at 20,000*g* for 30 min. Supernatants were applied into the GSTrap FF column (GE Healthcare, Piscataway, NJ), pre-equilibrated with sonication buffer, and washed twice with bed volume of the sonication buffer. The bound glutathione *S*-transferase (GST) fusion proteins were eluted from the column using sonication buffer containing 10 mM reduced glutathione. Eluted samples were desalted and concentrated using Vivaspin 6/10,000 MWCO (Vivascience AG, Hannover, Germany), and the protein concentrations were determined according to the method of Bradford. To cleave the bonds between tag GST protein and recombinant protein, GST fusion proteins were digested with PreScission Protease (GE Healthcare) in the presence of PreScission Protease buffer (50 mM Tris–HCl, 150 mM NaCl, 1 mM EDTA, 1 mM DTT, pH 7.0) at 4 °C for 16 h.

5.3. Assay for the RNA N-glycosidase (RNG) activity

Ribosomes from rat liver and *E. coli* JM109 were used as eukaryotic and prokaryotic ribosomes, respectively. These ribosomes were prepared under RNase-free conditions as described previously (Kondo et al., 2002). The RNG activity was assayed according to the method of Endo et al. (1987). Briefly, ribosomes were incubated with recombinant proteins at 37 °C for 30 min in 30 μl reaction buffer (25 mM Tri–HCl, 50 mM KCl, 5 mM $MgCl_2$, pH 7.6). rRNA incubated in the absence of recombinant proteins served as a negative control. After incubation, the rRNA in the reaction mixture was extracted using phenol–chloroform and precipitated with EtOH. The extracted RNA was incubated with 1 M aniline acetate (pH 4.5) at 37 °C for 15 min and precipitated with EtOH. The rRNA was subjected to electrophoresis in a 3.5% (w/v) polyacrylamide gel containing 7 M urea and visualized by staining with ethidium bromide. The extent of RNG activity was calculated from linear regression of the log of RIP concentration against the band intensity of a specific RNA fragment (α-fragment) released from aniline-treated rRNA in PAGE gel using NIH Image software (ver. 1.62, National Institutes of Health, USA). The band intensities of 5.8S rRNA and 5S rRNA were used as internal standards for eukaryotic and prokaryotic ribosomes, respectively.

Acknowledgements

The authors are grateful to Professor Dr. H. Umeyama of Kitasato University for technical advice and scientific discussions.

References

Barbieri, L., Battelli, M.G., Stirpe, F., 1993. Ribosome-inactivating proteins from plants. Biochim. Biophys. Acta 1154, 237–282.

Baykal, U., Tumer, N.E., 2007. The C-terminus of pokeweed antiviral protein has distinct roles in transport to the cytosol, ribosome depurination and cytotoxicity. Plant J. 49, 995–1007.

Chaddock, J.A., Monzingo, A.F., Robertus, J.D., Lord, J.M., Roberts, L.M., 1996. Major structural differences between pokeweed antiviral protein and ricin A-chain do not account for their differing ribosome specificity. Eur. J. Biochem. 235, 159–166.

Ek, O., Waurzyniak, B., Myers, D.E., Uckun, F.M., 1998. Antitumor activity of TP3(anti-p80)-pokeweed antiviral protein immunotoxin in hamster cheek pouch and severe combined immunodeficient mouse xenograft models of human osteosarcoma. Clin. Cancer Res. 4, 1641–1647.

Endo, Y., Mitsui, K., Motizuki, M., Tsurugi, K., 1987. The mechanism of action of ricin and related toxic lectins on eukaryotic ribosomes. The site and the characteristics of the modification in 28S ribosomal RNA caused by the toxins. J. Biol. Chem. 262, 5908–5912.

Endo, Y., Tsurugi, K., 1987. RNA *N*-glycosidase activity of ricin A-chain. Mechanism of action of the toxic lectin ricin on eukaryotic ribosomes. J. Biol. Chem. 262, 8128–8130.

Endo, Y., Tsurugi, K., 1988. The RNA *N*-glycosidase activity of ricin A-chain. The characteristics of the enzymatic activity of ricin A-chain with ribosomes and with rRNA. J. Biol. Chem. 263, 8735–8739.

Frankel, A., Welsh, P., Richardson, J., Robertus, J.D., 1990. Role of arginine 180 and glutamic acid 177 of ricin toxin A chain in enzymatic inactivation of ribosomes. Mol. Cell Biol. 10, 6257–6263.

Girbés, T., Ferreras, J.M., Arias, F.J., Stirpe, F., 2004. Description, distribution, activity and phylogenetic relationship of ribosome-inactivating proteins in plants, fungi and bacteria. Mini Rev. Med. Chem. 4, 461–476.

Hartley, M.R., Legname, G., Osborn, R., Chen, Z., Lord, J.M., 1991. Single-chain ribosome inactivating proteins from plants depurinate *Escherichia coli* 23S ribosomal RNA. FEBS Lett. 290, 65–68.

Hudak, K.A., Parikh, B.A., Di, R., Baricevic, M., Santana, M., Seskar, M., Tumer, N.E., 2004. Generation of pokeweed antiviral protein mutations in *Saccharomyces cerevisiae*: evidence that ribosome depurination is not sufficient for cytotoxicity. Nucleic Acid Res. 32, 4244–4256.

Irvin, J.D., 1975. Purification and partial characterization of the antiviral protein from *Phytolacca americana* which inhibits eukaryotic protein synthesis. Arch. Biochem. Biophys. 169, 522–528.

Kondo, T., Yoshikawa, T., Ogihara, Y., Mizukami, H., 2002. Fusion with maltose-binding protein (MBP) affects neither RNA *N*-glycosidase activity nor immunogenicity of karasurin-A, ribosome-inactivating protein from *Trichosanthes kirilowii* var. *japonica*. Biothechonol. Lett. 24, 1117–1124.

Mizukami, H., Iida, K., Ogihara, Y., Kondo, T., Yoshikawa, T., 2001. Cloning and bacterial expression of karasurins, ribosome-inactivating proteins (RIPs) from *Tricosanthes kirilowii* var. *japonica*. Plant Biotechnol. 55, 301–303.

Moazed, D., Robertson, J.M., Noller, H.F., 1988. Interaction of elongation factors EF-G and EF-Tu with a conserved loop in 23S RNA. Nature 334, 362–364.

Montfort, W., Villafranca, J.E., Monzingo, A.F., Ernst, S.R., Katzin, B., Rutenber, E., Xuong, N.H., Hamlin, R., Robertus, J.D., 1987. The three-dimensional structure of ricin at 2.8 Å. J. Biol. Chem. 262, 5398–5403.

Monzingo, A.F., Robertus, J.D., 1992. X-ray analysis of substrate analogs in the ricin A-chain active site. J. Mol. Biol. 227, 1136–1145.

Monzingo, A.F., Collins, E.J., Ernst, S.R., Irvin, J.D., Robertus, J.D., 1993. The 2.5 Å structure of pokeweed antiviral protein. J. Mol. Biol. 233, 705–715.

Olsnes, S., 2004. The history of ricin, abrin and related toxins. Toxicon 44, 361–370.

Parikh, B.A., Tumer, N.E., 2004. Antiviral activity of ribosome inactivating proteins in medicine. Mini Rev. Med. Chem. 4, 523–543.

Peumans, W.J., Hao, Q., Van Damme, E.J., 2001. Ribosome-inactivating proteins from plants: more than RNA *N*-glycosidases? FASEB J. 15, 1493–1506.

Qi, L., Nett, T.M., Allen, M.C., Sha, X., Harrison, G.S., Frederick, B.A., Crawford, E.D., Glode, L.M., 2004. Binding and cytotoxicity of conjugated and recombinant fusion proteins targeted to the gonadotropin-releasing hormone receptor. Cancer Res. 64, 2090–2095.

Rajamohan, F., Ozer, Z., Mao, C., Uckun, F.M., 2001. Active center cleft residues of pokeweed antiviral protein mediate its high-affinity binding to the ribosomal protein L3. Biochemistry 40, 9104–9114.

Ready, M.P., Katzin, B.J., Robertus, J.D., 1988. Ribosome-inhibiting proteins, retroviral reverse transcriptases, and RNase H share common structural elements. Proteins 3, 53–59.

Ready, M.P., Kim, Y., Robertus, J.D., 1991. Site-directed mutagenesis of ricin A-chain and implications for the mechanism of action. Proteins 10, 270–278.

Reinbothe, S., Reinbothe, C., Lehmann, J., Becker, W., Apel, K., Parthier, B., 1994. JIP60, a methyl jasmonate-induced ribosome-inactivating protein involved in plant stress reactions. Proc. Natl. Acad. Sci. USA 91, 7012–7016.

Robertus, J., 1991. The structure and action of ricin, a cytotoxic *N*-glycosidase. Semin. Cell Biol. 2, 23–30.

Toyokawa, S., Takeda, T., Ogihara, Y., 1991. Isolation and characterization of a new abortifacient protein, karasurin, from root tubers of *Trichosanthes kirilowii* Max. var. *japonicum* Kitam. Chem. Pharm. Bull. 39, 716–719.

Uckun, F.M., Bellomy, K., O'Neill, K., Messinger, Y., Johnson, T., Chen, C.L., 1999. Toxicity, biological activity, and pharmacokinetics of TXU (anti-CD7)-pokeweed antiviral protein in chimpanzees and adult patients infected with human immunodeficiency virus. J. Pharmacol. Exp. Ther. 291, 1301–1307.

Zarling, J.M., Moran, P.A., Haffar, O., Sias, J., Richman, D.D., Spina, C.A., Myers, D.E., Kuebelbeck, V., Ledbetter, J.A., Uckun, F.M., 1990. Inhibition of HIV replication by pokeweed antiviral protein targeted to $CD4^+$ cells by monoclonal antibodies. Nature 347, 92–95.